



Analytic Solution for a Non-axisymmetric Isothermal Dendrite

**G. B. McFadden
S.R. Coriell**

U.S. DEPARTMENT OF COMMERCE
Technology Administration
National Institute of Standards
and Technology
Gaithersburg, MD 20899-3890, USA

R. F. Sekerka

University Professor
Physics and Mathematics
Carnegie Mellon University
Pittsburgh, PA 15213-3890, USA

QC100
.U56
#6308
1999

Analytic Solution for a Non-axisymmetric Isothermal Dendrite

G. B. McFadden
S.R. Coriell

U.S. DEPARTMENT OF COMMERCE
Technology Administration
National Institute of Standards
and Technology
Gaithersburg, MD 20899-3890, USA

R. F. Sekerka

University Professor
Physics and Mathematics
Carnegie Mellon University
Pittsburgh, PA 15213-3890, USA

March 1999



U.S. DEPARTMENT OF COMMERCE
William M. Daley, Secretary

TECHNOLOGY ADMINISTRATION
Gary R. Bachula, Acting Under Secretary
for Technology

NATIONAL INSTITUTE OF STANDARDS
AND TECHNOLOGY
Raymond G. Kammer, Director

Analytic Solution for a Non-Axisymmetric Isothermal Dendrite

G. B. McFadden^{a,*}, S. R. Coriell^a, R. F. Sekerka^b

^aNational Institute of Standards and Technology
Gaithersburg, MD 20899-8910, USA

^bUniversity Professor, Physics and Mathematics
Carnegie Mellon University
Pittsburgh, PA 15213-3890, USA

Abstract

The Ivantsov solution for an isothermal paraboloid of revolution growing into a pure, supercooled melt provides a relation between the bulk supercooling and a dimensionless product (the Peclet number P) of the growth velocity and tip radius of a dendrite. Horvay and Cahn generalized this axisymmetric analytical solution to a paraboloid with elliptical cross-section. They found that as the deviation of the dendrite cross-section from a circle increases, the two-fold symmetry of the interface shape causes a systematic deviation from the supercooling/Peclet number relation of the Ivantsov solution. To model dendritic growth in cubic materials, we find approximate solutions for paraboloids having perturbations with four-fold axial asymmetry. These solutions are valid through second order in the perturbation amplitude, and provide self-consistent corrections through this order to the supercooling/Peclet number relation of the Ivantsov solution. Glicksman and colleagues have measured the shape and the supercooling/Peclet number relation for growth of succinonitrile dendrites in microgravity. For a Peclet number of $P \approx 0.004$ and the experimentally observed shape, we calculate a correction corresponding to a 9% increase in the supercooling, in general agreement with the experimental results.

PACS: 81.10.Aj, 64.70.Dv, 66.10.Cb, 81.10.Mx

Keywords: dendritic growth, supercooled liquids, non-axisymmetric dendrites, Ivantsov relation

*Corresponding author. Fax + 1 301 990-4127; e-mail: mcfadden@nist.gov

1 Introduction

For a number of years there have been extensive measurements directed toward an understanding of dendritic growth from pure supercooled melts [1–5]. Of primary interest has been a comparison with theory of the dependence of the growth speed, V , and the tip radius, ρ , on the supercooling, ΔT . One ingredient of the theoretical basis for this comparison is the Ivantsov solution [6], which is an exact solution for the steady-state growth of an isothermal semi-infinite paraboloid of revolution. This solution results in a relationship of the form

$$S = Pe^P E_1(P), \quad (1)$$

where $S = c_V \Delta T / L_V$ is the Stefan number (dimensionless supercooling), $P = V\rho / 2\kappa$ is the Peclet number, and $E_1(P)$ is the exponential integral (see Eq. (14)); here, c_V is the heat capacity per unit volume, L_V is the latent heat per unit volume, and κ is the thermal diffusivity. For this solution the solid is isothermal and is assumed to have the same density as the liquid. The supercooling is $\Delta T = T_M - T_\infty$, where T_M is the melting point and T_∞ is the temperature of the supercooled liquid far from the paraboloid. The second theoretical ingredient has been a value of the selection parameter $\sigma^* = 2d_0\kappa / V\rho^2$, where $d_0 = \gamma T_M c_V / L_V^2$ is a capillary length based on the surface tension γ . Values of σ^* have been calculated from considerations of marginal stability [1,7] and from the theory of microscopic solvability [8–14]. Recently, Glicksman et al. [2] have performed very careful measurements of the dendritic growth of pure succinonitrile (SCN) in microgravity in order to reduce fluid convection and thus to conduct a stringent test of the above relationships. For measurements down to supercoolings of 0.05 K ($S = 0.002$), reasonable agreement is obtained with $\sigma^* \approx 0.02$. Independent of selection, there appears to be a systematic discrepancy from the Ivantsov relation given by Eq. (1). For supercoolings between 0.5 K and 1 K, the measured supercooling for a given Peclet number is about 10% higher than would be predicted by Eq. (1); see Fig. 6 of Ref. [2]. Some possible reasons for this discrepancy are the effect of finite container size, thermal fields due to other dendrites, and deviations of shape from a paraboloid of revolution. Previous theoretical studies of the effects of the dendrite geometry on the surrounding thermal field include boundary integral computations by Schaefer [15]; this work has recently been extended by LaCombe [16]. These studies indicate how the temperature

field near the dendrite tip is influenced by latent heat emission from the dendrite surface at various distances from the tip.

In the present paper, we investigate the effect of a specific deviation of shape from a paraboloid of revolution, namely a paraboloid with a perturbation having n -fold symmetry about the growth axis. The possible importance of such a perturbation is suggested by the measurements of Glicksman et al. [3] of anisotropic tip shapes that can be fit by functions of the form

$$\frac{z}{\rho} = \frac{1}{2} - \frac{1}{2} \left(\frac{r}{\rho} \right)^2 - Q(\phi) \left(\frac{r}{\rho} \right)^4, \quad (2)$$

where r , z , and ϕ are cylindrical coordinates with growth along the positive z axis. The function $Q(\phi)$ has four-fold symmetry, and to a crude approximation is given by $Q(\phi) \approx Q_0 \cos 4\phi$, where Q_0 is a constant.

A more general exact solution for steady-state solidification into a supercooled melt is that of Horvay and Cahn for an elliptical paraboloid [17]. For this solution the relationship between S and P depends on an additional parameter b that characterizes the eccentricity of the elliptical cross-section. Such a body has two-fold axial anisotropy. This result suggests that a paraboloid having a perturbation with n -fold axial symmetry would also have a relationship between S and P that depends upon the amplitude of the perturbation. We proceed to obtain such a solution for $n = 3$ and $n = 4$ by means of an expansion to second order in the perturbation amplitude, necessary because the first order correction vanishes by symmetry. Dendrites with n -fold symmetry about a preferred growth direction generally occur because of the presence of anisotropy in surface tension or interface attachment kinetics. For a cubic material, dendritic growth in the [100] direction leads to shapes with four-fold symmetry, and growth in the [111] direction leads to shapes with three-fold symmetry. The vast majority of quantitative data exist for dendrites with four-fold symmetry [1], although there have been observations of three-fold shapes in solution growth [18] and in solid-state order-disorder transitions [19]. In addition to the possible application of our results to observations of growth with three-fold symmetry, the analysis for the case $n = 3$ is also included to facilitate our understanding of the solution technique, with is based on extending the known results for the two-fold Horvay-Cahn solution to the more difficult case of four-fold symmetry.

The main results of the paper may be summarized as follows. In cylindrical coordinates, we

show that the four-fold dendrite tip has the form

$$\frac{z}{\rho} = \frac{1}{2} - \frac{1}{2} \left(\frac{r}{\rho} \right)^2 - \frac{\epsilon}{2} \cos 4\phi \left(\frac{r}{\rho} \right)^4 + \frac{\epsilon^2}{2} \left[\alpha(P) \left(\frac{r}{\rho} \right)^4 + \beta(P) \left(\frac{r}{\rho} \right)^6 \right] + O(\epsilon^3), \quad (3)$$

where ϵ represents the amplitude of the four-fold perturbation to the axisymmetric paraboloid. The corresponding correction to the relation (1) is found to have the form

$$S = Pe^P E_1(P) + \frac{\epsilon^2}{2} S^{(2)}(P) + O(\epsilon^3). \quad (4)$$

The specific dependence of the coefficients α and β , and the correction $S^{(2)}$, on Peclet number are worked out in detail. The measurements of Glicksman et al. for succinonitrile at $P \approx 0.004$ correspond to a value $\epsilon = -0.008$, and the term $\epsilon^2 S^{(2)}/2$ represents a 9 % increase in S .

2 Governing Equations

We use parabolic coordinates to describe the dendritic growth. The coordinate system is fixed in the dendrite tip's frame of reference, so that with regard to the laboratory frame in which the crystal is at rest, the moving coordinate system has constant velocity V . The relations between the parabolic coordinates (ξ, η, ϕ) and the Cartesian coordinates (x, y, z) are [20]

$$x = \xi\eta \cos \phi, \quad (5)$$

$$y = \xi\eta \sin \phi, \quad (6)$$

$$z = \frac{1}{2}(\xi^2 - \eta^2). \quad (7)$$

For a steady-state isothermal dendrite growing in the z -direction, we express the surface of the dendrite in the form $\xi = f(\eta, \phi)$. The range of variables is taken to be $f(\eta, \phi) \leq \xi < \infty$, $0 \leq \eta < \infty$, and $0 \leq \phi < 2\pi$ in the liquid, and $0 \leq \xi \leq f(\eta, \phi)$, $0 \leq \eta < \infty$, and $0 \leq \phi < 2\pi$ in the solid, which is isothermal.

The equation for the steady-state temperature T in the liquid,

$$0 = \kappa \nabla^2 T + V \frac{\partial T}{\partial z}, \quad (8)$$

becomes, in the parabolic coordinate system,

$$0 = \kappa \left(\frac{\partial^2 T}{\partial \xi^2} + \frac{\partial^2 T}{\partial \eta^2} \right) + \kappa \left(\frac{1}{\xi} \frac{\partial T}{\partial \xi} + \frac{1}{\eta} \frac{\partial T}{\partial \eta} \right) + \frac{\kappa H^2}{\xi^2 \eta^2} \frac{\partial^2 T}{\partial \phi^2} + V \left(\xi \frac{\partial T}{\partial \xi} - \eta \frac{\partial T}{\partial \eta} \right), \quad (9)$$

where $H = \sqrt{\eta^2 + \xi^2}$. The heat flux boundary condition $-Lv_n = k\partial T/\partial n$ becomes

$$-LV(f + \eta f_\eta) = k \left(\frac{\partial T}{\partial \xi} - f_\eta \frac{\partial T}{\partial \eta} - \frac{H^2 f_\phi}{\eta^2 f^2} \frac{\partial T}{\partial \phi} \right), \quad (10)$$

where $k = c_V \kappa$ is the thermal conductivity. The solid-liquid interface is assumed to be isothermal at the melting temperature, T_M ; i.e., we neglect the effects of capillarity. The liquid far from the interface is supercooled to a temperature $T_\infty < T_M$, so that $T(\xi, \eta, \phi) \rightarrow T_\infty$ as $\xi \rightarrow \infty$.

2.1 Dimensionless Formulation

We take $2\kappa/V$ to be the length scale, and measure temperature relative to the melting point in units of $(T_M - T_\infty)$. The dimensionless governing equations then become (retaining the same notation henceforth)

$$0 = \frac{\partial^2 T}{\partial \xi^2} + \frac{\partial^2 T}{\partial \eta^2} + \frac{1}{\xi} \frac{\partial T}{\partial \xi} + \frac{1}{\eta} \frac{\partial T}{\partial \eta} + \frac{H^2}{\xi^2 \eta^2} \frac{\partial^2 T}{\partial \phi^2} + 2\xi \frac{\partial T}{\partial \xi} - 2\eta \frac{\partial T}{\partial \eta}. \quad (11)$$

At the interface we have $T = 0$ and

$$-(f + \eta f_\eta) = \frac{S}{2} \left\{ \frac{\partial T}{\partial \xi} - f_\eta \frac{\partial T}{\partial \eta} - \frac{H^2 f_\phi}{\eta^2 f^2} \frac{\partial T}{\partial \phi} \right\}. \quad (12)$$

In the far-field we have $T(\xi, \eta, \phi) \rightarrow -1$ as $\xi \rightarrow \infty$.

3 Ivantsov Solution

The Ivantsov solution, which we denote by a superscript '(0)', has isotherms corresponding to $\xi = \text{constant}$, and a solid-liquid interface $f^{(0)} = \xi_0$. The surface of the dendrite for this solution is given by the equation $z = \frac{1}{2}(\xi_0^2 - r^2/\xi_0^2)$, where $r^2 = x^2 + y^2$. The dimensionless

tip radius computed from the above expression is $\xi_0^2 = V\rho/2\kappa = P$. The Ivantsov solution is

$$T^{(0)}(\xi) = \frac{[E_1(\xi^2) - E_1(P)]}{E_1(P)}, \quad (13)$$

where

$$E_1(u) = \int_u^\infty \frac{e^{-t}}{t} dt, \quad (14)$$

is the exponential integral [21]. The boundary condition (12) results in Eq. (1), which we now write $S^{(0)} = P e^P E_1(P)$.

4 Horvay-Cahn Two-Fold Solution

Horvay and Cahn [17] generalized the Ivantsov solution to obtain a model of an isothermal dendrite that has an elliptical cross-section. The isotherms correspond to constant values of ω , where

$$\frac{x^2}{\omega - b} + \frac{y^2}{\omega + b} = \omega - 2z, \quad (15)$$

and the interface corresponds to $\omega = P$. Here b determines the aspect ratio of the elliptical cross-section of the dendrite. For $b = 0$ the cross-section is circular; we will assume $|b| < P$. Eq. (15) is actually a symmetrized version of the corresponding expression given by Horvay and Cahn, with dimensionless radii of curvature $(P - b)$ in the x - z plane and $(P + b)$ in the y - z plane. Thus, the average dimensionless radius of curvature is P . The thermal field is given by

$$T(\omega) = \frac{[G(\omega) - G(P)]}{G(P)} \quad (16)$$

where

$$G(\omega) = \int_\omega^\infty \frac{e^{-t}}{\sqrt{t^2 - b^2}} dt \quad (17)$$

and

$$S = \sqrt{P^2 - b^2} e^P G(P). \quad (18)$$

For $b = 0$, $G(P) = E_1(P)$ and one recovers the Ivantsov relation (1).

4.1 The Horvay-Cahn Solution in Parabolic Coordinates

To gain insight into solutions with four-fold symmetry, we re-express the two-fold Horvay-Cahn solution in the parabolic coordinate system (ξ, η, ϕ) , to obtain

$$\xi^2 \eta^2 \left[\frac{\cos^2 \phi}{\omega - b} + \frac{\sin^2 \phi}{\omega + b} \right] = \omega - (\xi^2 - \eta^2), \quad (19)$$

which defines implicitly the function $\omega = \omega(\xi, \eta, \phi)$. The temperature field has the form

$$T(\xi, \eta, \phi) = \frac{[G(\omega(\xi, \eta, \phi)) - G(P)]}{G(P)}. \quad (20)$$

The interface shape can be obtained from the relation $\omega(\xi, \eta, \phi) = P$, which implicitly defines the function $\xi = f(\eta, \phi)$; i.e.,

$$f^2 \eta^2 \left[\frac{\cos^2 \phi}{P - b} + \frac{\sin^2 \phi}{P + b} \right] = P - (f^2 - \eta^2). \quad (21)$$

4.2 Perturbation Expansion of the Horvay-Cahn Solution

From Eq. (21) we see that the ellipticity of the shape depends on the ratio $(P - b)/(P + b)$. In order to study a shape of fixed ellipticity, we make this ratio independent of P by writing $b = P\epsilon$, where $|\epsilon| < 1$. We proceed to expand the Horvay-Cahn solution in powers of ϵ for $|\epsilon| \ll 1$. More specifically, we expand in ϵ while keeping the Peclet number fixed, which keeps the interface tip at $z = P/2$ and also fixes the average radius of curvature. Thus

$$\begin{pmatrix} T(\eta, \xi, \phi, \epsilon) \\ f(\eta, \phi, \epsilon) \\ S(\epsilon) \end{pmatrix} = \begin{pmatrix} T^{(0)}(\xi) \\ \xi_0 \\ S^{(0)} \end{pmatrix} + \epsilon \begin{pmatrix} T^{(1)}(\eta, \xi, \phi) \\ f^{(1)}(\eta, \phi) \\ S^{(1)} \end{pmatrix} + \frac{\epsilon^2}{2} \begin{pmatrix} T^{(2)}(\eta, \xi, \phi) \\ f^{(2)}(\eta, \phi) \\ S^{(2)} \end{pmatrix} + O(\epsilon^3) \quad (22)$$

where the leading order terms correspond to the Ivantsov solution. The first order solution is

$$T^{(1)}(\xi, \eta, \phi) = \frac{-P}{E_1(P)} \frac{e^{-\xi^2}}{(\xi^2 + \eta^2)} \left(\frac{\eta^2}{\xi^2} \right) \cos 2\phi \quad (23)$$

$$f^{(1)}(\eta, \phi) = \frac{-P^{1/2} \eta^2 \cos 2\phi}{2(P + \eta^2)} \quad (24)$$

$$S^{(1)} = 0 \quad (25)$$

which illustrates explicitly the two-fold symmetry.

The second order solution is

$$T^{(2)}(\xi, \eta, \phi) = \frac{-P^2}{4E_1(P)} \frac{\partial}{\partial z} \left[\frac{e^{-\xi^2} \cos 4\phi}{(\xi^2 + \eta^2)} \left(\frac{\eta}{\xi} \right)^4 \right] + \frac{P^2}{8E_1(P)} \frac{\partial^2}{\partial z^2} E_1(\xi^2) + \frac{P^2}{2E_1(P)} \frac{\partial}{\partial z} E_1(\xi^2) - \frac{e^{-P}}{2[E_1(P)]^2} (1-P) E_1(\xi^2) \quad (26)$$

$$f^{(2)}(\eta, \phi) = \frac{-P^{1/2} \eta^2}{(P + \eta^2)} + \frac{3P^{1/2} \eta^4 \cos^2(2\phi)}{4(P + \eta^2)^2} \quad (27)$$

$$S^{(2)} = P e^P E_1(P) \left[\frac{P^2}{2} - 1 \right] + \frac{P}{2} (1 - P), \quad (28)$$

where $H^2 \partial / \partial z = (\xi \partial / \xi - \eta \partial / \eta)$. We have written Eq. (26) in terms of $E_1(\xi^2)$, which is the zeroth order solution to Eq. (11), and its first and second partial derivatives with respect to z , which expressions also satisfy Eq. (11). Thus the first term also satisfies Eq. (11), as is discussed further in the Appendix.

Note that the first non-vanishing correction to the supercooling due to the two-fold interface perturbation is quadratic in the amplitude of the perturbation. The fact that $S^{(1)} = 0$ can be understood by realizing that the relationship between S and P must not depend on the sign of the interface perturbation because changing the sign would simply interchange x and y . For large Peclet numbers, $S^{(2)}$ has the expansion

$$S^{(2)} = \frac{-2}{P} + \frac{10}{P^2} + O\left(\frac{1}{P^3}\right). \quad (29)$$

In Fig. 1 we plot the quantity $S^{(2)}/S^{(0)}$ as a function of Peclet number over the range $10^{-5} < P < 10$. The correction $S^{(2)}$ is negative, and becomes smaller in magnitude as the Peclet number increases. In Fig. 2 we plot the ratio $S/S^{(0)}$ as a function of ϵ for a Peclet number of $P = 0.01$. The solid curve corresponds to the exact value of S as given by Eq. (18), and the dashed line corresponds to the second order approximation. The approximate and exact results are in good agreement for $\epsilon < 1/2$.

5 Expansion Procedure for the n -Fold Solution

Guided by our expansion of the Horvay-Cahn solution, we use an expansion procedure to obtain solutions having n -fold symmetry. We consider an expansion having the form of

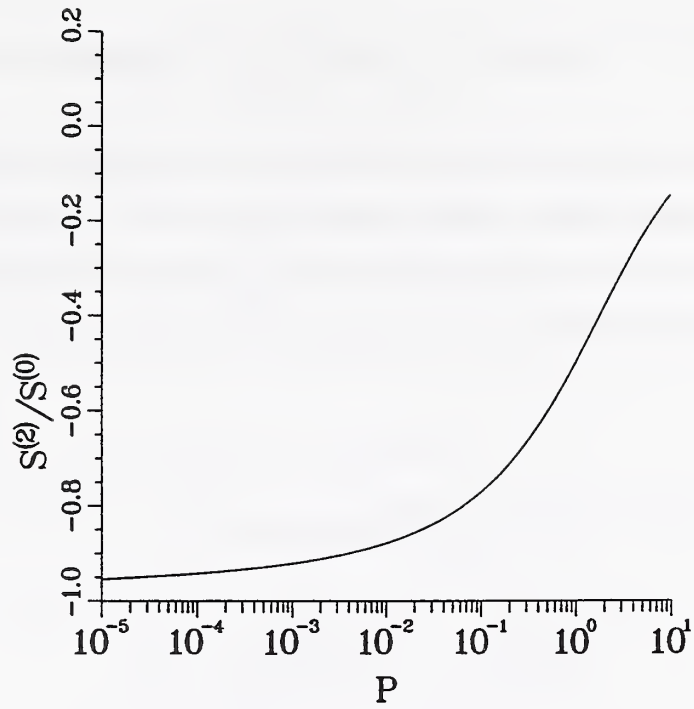


Figure 1: Plot of $S^{(2)}/S^{(0)}$ as a function of the Peclet number P for $n = 2$. The quantity $S^{(2)}$ gives the correction in supercooling due to a small departure from axial symmetry as described by Eq. (4).

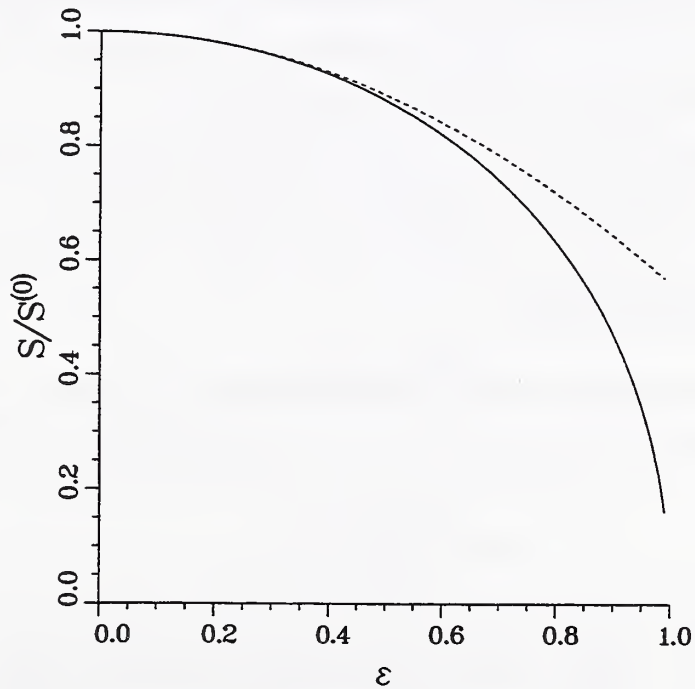


Figure 2: Plot of $S/S^{(0)}$ as a function of ϵ for a Peclet number of $P = 0.01$. The solid curve corresponds to the exact value of S , and the dashed line corresponds to the second order approximation with $S \approx S^{(0)} + \epsilon^2 S^{(2)}/2$.

Eq. (22). Since the heat equation is linear, each term $T^{(j)}$ in the expansion of the temperature satisfies Eq. (11).

We use a specific form for the function $f^{(1)}(\eta, \phi)$, proportional to $\cos n\phi$, which for $n = 2$ agrees with our expansion of the Horvay-Cahn solution, so that ϵ relates in the same way to the amplitude of an interface perturbation. We require that the position of the dendrite tip and the angular average of the radius of curvature of the tip remain fixed at their unperturbed values:

$$f(\eta, \phi, \epsilon)|_{\eta=0} = P^{1/2}, \quad (30)$$

$$\frac{1}{2\pi} \int_0^{2\pi} \rho(\phi, \epsilon) d\phi = P, \quad (31)$$

where

$$\rho(\phi, \epsilon) = \frac{[f(\eta, \phi, \epsilon)]^2}{[1 - f(\eta, \phi, \epsilon)f_{\eta\eta}(\eta, \phi, \epsilon)]} \Big|_{\eta=0} \quad (32)$$

is the radius of curvature of the tip in a section $\phi = \text{constant}$. This allows us to focus on the dependence of S on ϵ for a fixed value of P . We have

$$\rho(\phi, \epsilon) = P + \epsilon P^{3/2} f_{\eta\eta}^{(1)}(0, \phi) + \frac{\epsilon^2}{2} \left\{ P^{3/2} f_{\eta\eta}^{(2)}(0, \phi) + 2P^2 [f_{\eta\eta}^{(1)}(0, \phi)]^2 \right\} + O(\epsilon^3), \quad (33)$$

which when substituted into Eq. (31) gives to second order

$$0 = \frac{1}{2\pi} \int_0^{2\pi} \left\{ P^{1/2} f_{\eta\eta}^{(2)}(0, \phi) + 2P [f_{\eta\eta}^{(1)}(0, \phi)]^2 \right\} d\phi. \quad (34)$$

5.1 First-Order Solution

To first order in ϵ , the condition of an isothermal interface and the flux boundary condition Eq. (12) lead to the following conditions at the unperturbed interface $\xi = P^{1/2}$:

$$T^{(1)} + \frac{\partial T^{(0)}}{\partial \xi} f^{(1)} = 0; \quad (35)$$

$$-\left[f^{(1)} + \eta \frac{\partial f^{(1)}}{\partial \eta} \right] = \frac{S^{(0)}}{2} \left[\frac{\partial T^{(1)}}{\partial \xi} + \frac{\partial^2 T^{(0)}}{\partial \xi^2} f^{(1)} \right] + \frac{S^{(1)}}{2} \frac{\partial T^{(0)}}{\partial \xi}. \quad (36)$$

By using the results derived in the appendix, the first order solution is

$$T^{(1)}(\xi, \eta, \phi) = \frac{-P}{E_1(P)} \frac{e^{-\xi^2}}{(\xi^2 + \eta^2)} \left(\frac{\eta}{\xi} \right)^n \cos n\phi, \quad (37)$$

$$f^{(1)}(\eta, \phi) = \frac{-P^{3/2}}{2(P + \eta^2)} \left(\frac{\eta}{P^{1/2}} \right)^n \cos n\phi. \quad (38)$$

This solution satisfies the boundary conditions (35) and (36) and the auxiliary conditions (30) and (31) provided that $S^{(1)} = 0$. Thus, as for the two-fold solution, there is no first order correction to the Stefan number S , which is consistent with the fact that a change in the sign of ϵ is equivalent a rotation about the growth axis through an angle π/n .

5.2 Second-Order Solution

At second order the isothermal condition and the flux boundary condition are

$$T^{(2)} + 2\frac{\partial T^{(1)}}{\partial \xi} f^{(1)} + \frac{\partial^2 T^{(0)}}{\partial \xi^2} (f^{(1)})^2 + \frac{\partial T^{(0)}}{\partial \xi} f^{(2)} = 0 \quad (39)$$

and

$$\begin{aligned} - \left[f^{(2)} + \eta \frac{\partial f^{(2)}}{\partial \eta} \right] &= \frac{S^{(2)}}{2} \frac{\partial T^{(0)}}{\partial \xi} + \frac{S^{(0)}}{2} \left[\frac{\partial T^{(2)}}{\partial \xi} + 2 \frac{\partial^2 T^{(1)}}{\partial \xi^2} f^{(1)} \right. \\ &+ \left. \frac{\partial^3 T^{(0)}}{\partial \xi^3} (f^{(1)})^2 + \frac{\partial^2 T^{(0)}}{\partial \xi^2} f^{(2)} - 2 \frac{\partial f^{(1)}}{\partial \eta} \frac{\partial T^{(1)}}{\partial \eta} - \frac{2H^2}{\eta^2 [f^{(0)}]^2} \frac{\partial f^{(1)}}{\partial \phi} \frac{\partial T^{(1)}}{\partial \phi} \right]. \end{aligned} \quad (40)$$

The solution for $n = 2, 3$, and 4 will be found in the form

$$T^{(2)} = a_0 \frac{\partial}{\partial z} \left[\frac{e^{-\xi^2} \cos 2n\phi}{(\xi^2 + \eta^2)} \left(\frac{\eta}{\xi} \right)^{2n} \right] + \sum_{j=-(n-2)}^2 b_j \frac{\partial^j}{\partial z^j} E_1(\xi^2), \quad (41)$$

where negative indices refer to ‘‘antiderivatives,’’ defined so that for $k > 0$,

$$w = \frac{\partial^{-k}}{\partial z^{-k}} E_1(\xi^2) \quad (42)$$

is equivalent to

$$E_1(\xi^2) = \frac{\partial^k w}{\partial z^k} \quad (43)$$

with $w \rightarrow 0$ as $z \rightarrow \infty$. Specific forms for the derivatives and antiderivatives that apply for $n \leq 4$ are given in the Appendix. The specific form of the coefficients b_j are found to depend on n , and in the following subsections we consider separately the two-fold, three-fold, and four-fold solutions at second order in the perturbation amplitude. In each case, however, the non-axisymmetric part of the solution, proportional to a_0 , is found to be given by the above

expression with the common value $a_0 = -P^2/[4E_1(P)]$.

Given the form (41) for $T^{(2)}$, we note that the form of $f^{(2)}$ then follows directly from the isothermal boundary condition (39), which yields

$$f^{(2)} = - \left[T^{(2)} + 2 \frac{\partial T^{(1)}}{\partial \xi} f^{(1)} + \frac{\partial^2 T^{(0)}}{\partial \xi^2} (f^{(1)})^2 \right] / \frac{\partial T^{(0)}}{\partial \xi}. \quad (44)$$

Thus, $f^{(2)}$ can also be expressed directly in terms of the set of coefficients a_0 and b_j .

5.3 Two-Fold Solution

Our analysis of the Horvay-Cahn solution, summarized in Eqs. (26)–(28), shows that the second order temperature $T^{(2)}$ of the two-fold solution can be expressed in the form (41) with $a_0 = -P^2/[4E_1(P)]$, $b_0 = -e^{-P}(1 - P)/(2[E_1(P)]^2)$, $b_1 = P^2/[2E_1(P)]$, and $b_2 = P^2/[8E_1(P)]$, with a correction $S^{(2)}$ given by Eq. (28).

We next shift our viewpoint, and consider how the constants a_0 , b_0 , b_1 , b_2 , and $S^{(2)}$ can be determined directly from the governing equations without making use of the closed form of the Horvay-Cahn solution. This will provide guidance in determining the general solution for dendrites having n -fold symmetry with $n > 2$.

Three linear equations are obtained by requiring that the flux boundary condition (40) is satisfied identically. Inserting the expressions (41) and (44) into the flux boundary condition results in an expression of the form

$$0 = \frac{(10P\eta^4 + 6\eta^6)E_1(P) \cos 4\phi}{P^{3/2}(P + \eta^2)^3} \left[a_0 + \frac{P^2}{4E_1(P)} \right] - \frac{4P^{1/2}(P - \eta^2)E_1(P)}{(P + \eta^2)^3} \left[b_2 - \frac{P^2}{8E_1(P)} \right] + P^{1/2} \left[b_0 E_1(P) \left\{ (1 + P)e^P E_1(P) - 1 \right\} - \frac{S^{(2)}}{Pe^P E_1(P)} - \frac{1}{2} \right]. \quad (45)$$

The angular dependence in the flux boundary condition is thus eliminated by the choice $a_0 = -P^2/[4E_1(P)]$. Similarly, the dependence on η is eliminated by choosing $b_2 = P^2/[8E_1(P)]$. Therefore, the last term provides a linear relation between $S^{(2)}$ and b_0 . We note that the term in $T^{(2)}$ that is proportional to b_1 simply represents an infinitesimal translation of the Ivantsov solution along the growth axis, so that the term $\partial E_1(\xi^2)/\partial z$ is a solution to the full set of linearized governing equations. The flux boundary condition is satisfied separately by this term, and b_1 does not appear in the resulting expression for the flux.

Two more equations are required for the determination of the expansion coefficients. An examination of the relation (44) between $f^{(2)}$ and $T^{(2)}$ for $\eta = 0$ shows that the condition (30) that fixes the tip position is equivalent to requiring that $T^{(2)}$ vanish at the tip. This provides a fourth linear equation

$$b_0 E_1(P) - 2b_1 \frac{e^{-P}}{P} + 4b_2 \frac{e^{-P}}{P^2} (P+1) = 0. \quad (46)$$

As noted above, the coefficient b_1 is associated with a translation of the dendrite along the growth axis, so that fixing the tip position is equivalent to determining the value of b_1 given values for the remaining coefficients.

A fifth equation results from the curvature condition (34), which for $n = 2$ yields

$$\frac{2b_1}{P^2} - \frac{8b_2}{P^3} (P+2) = \frac{-2}{PE_1(P)}. \quad (47)$$

We therefore obtain five independent linear equations for the determination of the expansion coefficients a_0 , b_0 , b_1 , and b_2 , and the correction $S^{(2)}$. It can then be checked directly that the solution to these linear equations reproduces the results of the second order expansion of the exact Horvay-Cahn solution given above.

5.4 Three-Fold Solution

We look for a three-fold ($n = 3$) second order solution having the form

$$\begin{aligned} T^{(2)}(\xi, \eta, \phi) = & a_0 \frac{\partial}{\partial z} \left[\frac{e^{-\xi^2} \cos 2n\phi}{(\xi^2 + \eta^2)} \left(\frac{\eta}{\xi} \right)^{2n} \right] \\ & + b_0 E_1(\xi^2) + b_1 \frac{\partial}{\partial z} E_1(\xi^2) + b_2 \frac{\partial^2}{\partial z^2} E_1(\xi^2) + b_{-1} u(\xi, \eta), \end{aligned} \quad (48)$$

where we have added to the form of the two-fold solution an additional solution $u(\xi, \eta)$ given by the “anti-derivative”

$$\frac{\partial}{\partial z} u(\xi, \eta) = E_1(\xi^2), \quad (49)$$

(see Appendix), which provides a solution with more rapid growth in η to balance the η -dependence generated by the non-axisymmetric part of the solution.

The condition (30) that the tip is fixed leads to

$$b_0 E_1(P) - 2b_1 \frac{e^{-P}}{P} + 4b_2 \frac{e^{-P}}{P^2} (P+1) + \frac{b_{-1}}{2} [P E_1(P) - e^{-P}] = 0. \quad (50)$$

The condition (31) that the curvature is fixed yields

$$\frac{2b_1}{P^2} - \frac{8b_2}{P^3} (P+2) + \frac{b_{-1}}{2} [1 - (P+1) E_1(P) e^P] = 0. \quad (51)$$

Inserting the expressions (44) and (48) into the flux boundary condition (40) gives

$$\begin{aligned} 0 = & \frac{(14P\eta^6 + 10\eta^8) E_1(P) \cos 6\phi}{P^{5/2} (P + \eta^2)^3} \left[a_0 + \frac{P^2}{4E_1(P)} \right] - \frac{4P^{1/2} (P - \eta^2) E_1(P)}{(P + \eta^2)^3} \left[b_2 + \frac{P^2}{8E_1(P)} \right] \\ & - \frac{P^{1/2} E_1(P) \eta^2}{2} \left[b_{-1} \left\{ e^P E_1(P) (P^2 + 4P + 2) - (P + 3) \right\} + \frac{4}{P E_1(P)} \right] \\ & + P^{1/2} \left[b_0 E_1(P) \left\{ (1 + P) e^P E_1(P) - 1 \right\} - \frac{S^{(2)}}{P e^P E_1(P)} + \frac{1}{2} \right. \\ & \left. + \frac{E_1(P) b_{-1}}{2} \left\{ P e^P E_1(P) (P + 2) - (P + 1) \right\} \right]. \end{aligned} \quad (52)$$

We note that the expression $b_{-1} u(\xi, \eta)$ in Eq. (48) is needed to balance the inhomogeneous term $4/[P E_1(P)]$ in the third term (proportional to η^2) in the above expression. The first three terms in this expression can be eliminated by choosing $a_0 = -P^2/[4E_1(P)]$, $b_2 = -P^2/[8E_1(P)]$, and

$$b_{-1} = \frac{-4}{P E_1(P) [(P^2 + 4P + 2) e^P E_1(P) - (P + 3)]}. \quad (53)$$

The remaining term in Eq. (52) then provides a linear equation relating $S^{(2)}$ and b_0 , which, in conjunction with (50) and (51), can be solved to provide the supercooling correction

$$\begin{aligned} S^{(2)} = & - \left\{ (P^5 + 8P^4 + 24P^3 + 24P^2 + 12P) e^{2P} [E_1(P)]^2 \right. \\ & - (2P^4 + 14P^3 + 36P^2 + 16P) e^P E_1(P) + (P^3 + 6P^2 + 13P - 4) \left. \right\} / \\ & \left\{ 2 \left[(P^2 + 4P + 2) e^P E_1(P) - (P + 3) \right] \right\}. \end{aligned} \quad (54)$$

In Fig. 3 we plot the quantity $PS^{(2)}/S^{(0)}$ as a function of Peclet number over the range

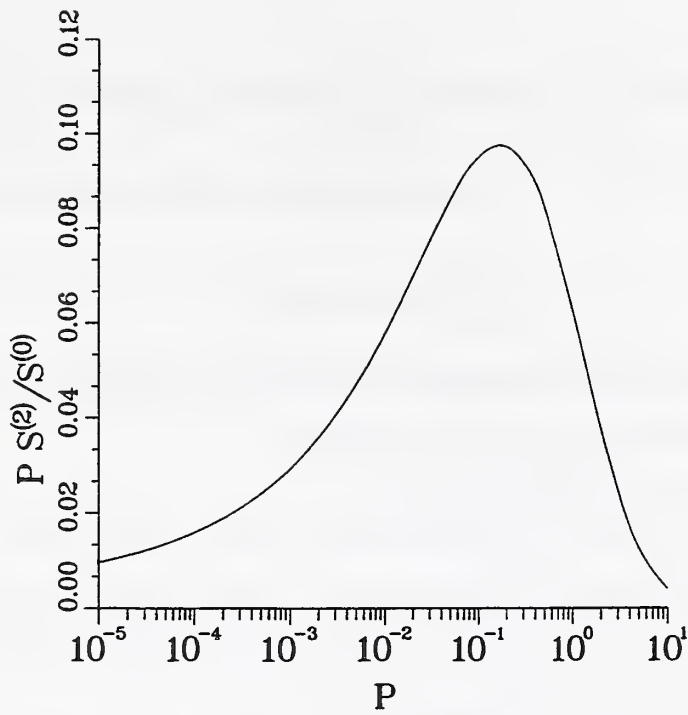


Figure 3: Plot of $PS^{(2)}/S^{(0)}$ as a function of the Peclet number P for $n = 3$.

$10^{-5} < P < 10$. The correction $S^{(2)}$ is positive for $n = 3$.

We note that the asymptotic expansion of $S^{(2)}$ for large P is given by

$$S^{(2)} = \frac{18}{P^4} - \frac{414}{P^5} + O\left(\frac{1}{P^6}\right). \quad (55)$$

Inserting the above values of the coefficients a_0 and b_j into expression (44) for the shape correction $f^{(2)}$ yields

$$f^{(2)} = \frac{-\eta^4 c_3(P)}{P + \eta^2} + \frac{5\eta^6 \cos^2(3\phi)}{4P^{1/2}(P + \eta^2)^2} \quad (56)$$

where

$$c_3(P) = \frac{e^P E_1(P)(6 + 18P + 9P^2 + P^3) - (11 + 8P + P^2)}{4\sqrt{P}[e^P E_1(P)(2 + 4P + P^2) - (3 + P)]}. \quad (57)$$

5.5 Four-Fold Solution

We look for a four-fold second order solution having the form

$$T^{(2)}(\xi, \eta, \phi) = a_0 \frac{\partial}{\partial z} \left[\frac{e^{-\xi^2} \cos 2n\phi}{(\xi^2 + \eta^2)} \left(\frac{\eta}{\xi} \right)^{2n} \right]$$

$$+ b_0 E_1(\xi^2) + b_1 \frac{\partial}{\partial z} E_1(\xi^2) + b_2 \frac{\partial^2}{\partial z^2} E_1(\xi^2) + b_{-1} u(\xi, \eta) + b_{-2} v(\xi, \eta), \quad (58)$$

where we have added to the form of the three-fold solution an additional solution given by the “anti-derivative”

$$\frac{\partial^2}{\partial z^2} v(\xi, \eta) = E_1(\xi^2), \quad (59)$$

(see Appendix), which provides an additional solution that is needed to balance terms generated by the non-axisymmetric part of the solution.

The condition that the tip is fixed leads to

$$b_0 E_1(P) - 2b_1 \frac{e^{-P}}{P} + 4b_2 \frac{e^{-P}}{P^2} (P+1) + \frac{b_{-1}}{2} [P E_1(P) - e^{-P}] + \frac{b_{-2}}{8} [P^2 E_1(P) + (1-P)e^{-P}] = 0. \quad (60)$$

The condition that the curvature is fixed yields

$$\frac{2b_1}{P^2} - \frac{8b_2}{P^3} (P+2) + \frac{b_{-1}}{2} [1 - (P+1)E_1(P)e^P] + \frac{b_{-2}}{4} [(P+1) - (P+2)P E_1(P)e^P] = 0. \quad (61)$$

Inserting the expressions (44) and (58) into the flux boundary condition (40) gives

$$\begin{aligned} 0 = & \frac{(18P\eta^8 + 14\eta^{10})E_1(P) \cos 8\phi}{P^{7/2}(P + \eta^2)^3} \left[a_0 + \frac{P^2}{4E_1(P)} \right] - \frac{4P^{1/2}(P - \eta^2)E_1(P)}{(P + \eta^2)^3} \left[b_2 - \frac{P^2}{8E_1(P)} \right] \\ & + \frac{P^{1/2}E_1(P)\eta^4}{16} \left[b_{-2} \left\{ e^P E_1(P)(P^3 + 9P^2 + 18P + 6) - (P^2 + 8P + 11) \right\} - \frac{72}{P^2 E_1(P)} \right] \\ & - \frac{P^{1/2}E_1(P)\eta^2}{4} \left[b_{-2} \left\{ e^P E_1(P)(p^3 + 6p^2 + 6p) - (p^2 + 5p + 2) \right\} \right. \\ & \quad \left. + 2b_{-1} \left\{ e^P E_1(P)(p^2 + 4p + 2) - (p + 3) \right\} - \frac{8}{P E_1(P)} \right] \\ & + P^{1/2} \left[b_0 E_1(P) \left\{ (1 + P)e^P E_1(P) - 1 \right\} - \frac{S^{(2)}}{P e^P E_1(P)} - \frac{1}{2} \right. \\ & \quad \left. + \frac{E_1(P)b_{-1}}{2} \left\{ P e^P E_1(P)(P + 2) - (P + 1) \right\} \right. \\ & \quad \left. + \frac{E_1(P)b_{-2}}{8} \left\{ P^2 e^P E_1(P)(P + 3) - (P^2 + 2P - 1) \right\} \right]. \quad (62) \end{aligned}$$

By zeroing the first four terms in this expression we find $a_0 = -P^2/[4E_1(P)]$, $b_2 = P^2/[8E_1(P)]$,

$$b_{-1} = 4[(P^4 - 36P^2 - 48P)e^P E_1(P) - (P^3 - P^2 - 34P - 18)]/$$

$$\left\{ P^2 E_1(P) [(P^5 + 13P^4 + 56P^3 + 96P^2 + 60P + 12)e^{2P} [E_1(P)]^2 \right.$$

$$\left. - 2(P^4 + 12P^3 + 45P^2 + 60P + 20)e^P E_1(P) + (P^3 + 11P^2 + 35P + 33) \right\}$$
(63)

and

$$b_{-2} = \frac{72}{P^2 E_1(P) [(P^3 + 9P^2 + 18P + 6)e^P E_1(P) - (P^2 + 8P + 11)]}. \quad (64)$$

The remaining term in Eq. (62) then provides a linear equation relating S^2 and b_0 , which, in conjunction with (60) and (61), can be solved to provide the supercooling correction

$$S^{(2)} = \left\{ (P^9 + 17P^8 + 114P^7 + 390P^6 + 672P^5 + 576P^4 + 144P^3 - 144P^2)e^{3P} [E_1(P)]^3 \right.$$

$$- (3P^8 + 48P^7 + 297P^6 + 908P^5 + 1254P^4 + 864P^3 + 372P^2)e^{2P} [E_1(P)]^2$$

$$+ (3P^7 + 45P^6 + 255P^5 + 685P^4 + 686P^3 + 470P^2 + 444P + 36)e^P E_1(P)$$

$$\left. - (P^6 + 14P^5 + 72P^4 + 166P^3 + 93P^2 + 136P + 126) \right\} /$$

$$\left\{ 2P [(P^5 + 13P^4 + 56P^3 + 96P^2 + 60P + 12)e^{2P} [E_1(P)]^2 \right.$$

$$- 2(P^4 + 12P^3 + 45P^2 + 60P + 20)e^P E_1(P)$$

$$\left. + (P^3 + 11P^2 + 35P + 33) \right\}$$
(65)

This expression should not be used to evaluate $S^{(2)}$ for large P in finite precision arithmetic, since considerable cancellation between large terms occurs that lead to a small result. Reliable results can be found by using extended precision in a symbolic arithmetic package. We note that the formal expansion of this expression for large Peclet number has the form

$$S^{(2)} = \frac{576}{P^6} - \frac{24192}{P^7} + O\left(\frac{1}{P^8}\right). \quad (66)$$

However, this expression requires very large Peclet numbers, on the order of $P \sim 1000$, to be useful.

In Fig. 4 we show the variation of the quantity $P^2 S^{(2)}/S^{(0)}$ over six orders of magnitude in

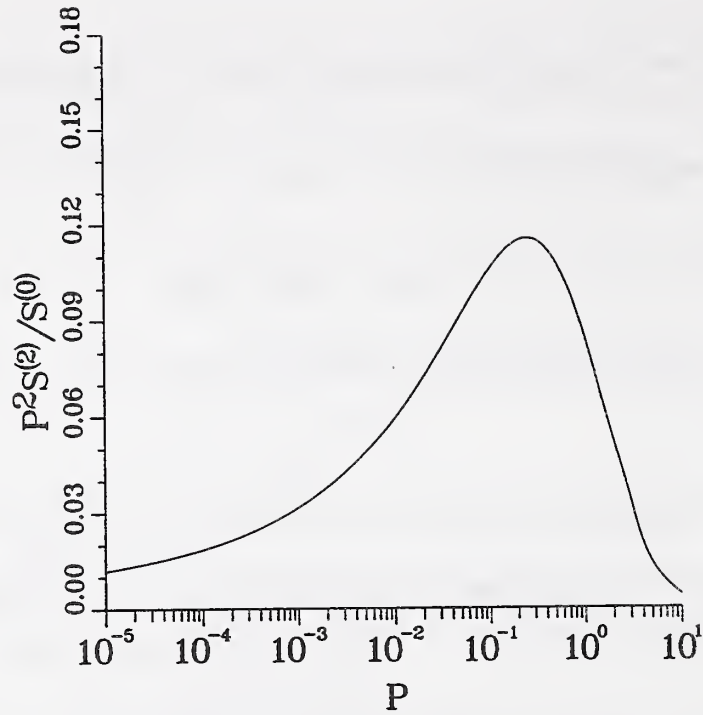


Figure 4: Plot of $P^2 S^{(2)}/S^{(0)}$ as a function of the Peclet number P for $n = 4$.

P . Over the range $10^{-5} < P < 0.1$ the results can be fit by a cubic polynomial in $\log_{10} P$, which has the form

$$S^{(2)} = \frac{S^{(0)}}{P^2} \left\{ 0.18490 + 9.3386 \times 10^{-2} [\log_{10} P] \right. \\ \left. + 1.7588 \times 10^{-2} [\log_{10} P]^2 + 1.1651 \times 10^{-3} [\log_{10} P]^3 \right\}, \quad (67)$$

which has a relative accuracy of within 2.5% over this range. In Fig. 5 we show the relative correction $S^{(2)}/S^{(0)}$ as a function of Peclet number. The relative correction is monotonically decreasing as a function of P .

Evaluating the expression (44) for $f^{(2)}$ with the above coefficients yields

$$f^{(2)} = \frac{-[\eta^6 d_4(P) - \eta^4 c_4(P)]}{e_4(P)(P + \eta^2)} + \frac{7 \eta^8 \cos^2(4\phi)}{4P^{3/2}(P + \eta^2)^2} \quad (68)$$

where

$$c_4(P) = P(144 + 432P + 648P^2 + 408P^3 + 126P^4 + 18P^5 + P^6)[e^P E_1(P)]^2$$

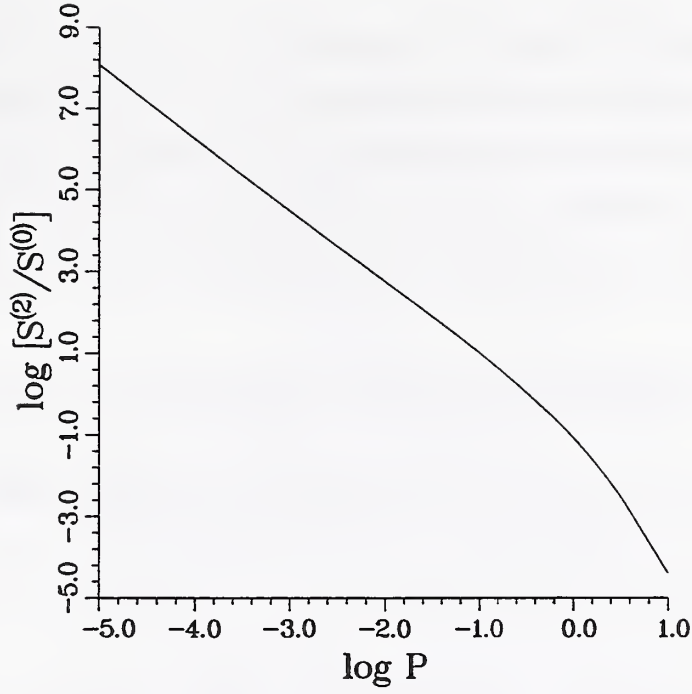


Figure 5: A log-log plot of the relative correction $S^{(2)}/S^{(0)}$ as a function of the Peclet number P for $n = 4$.

$$\begin{aligned}
& -2P(138 + 408P + 312P^2 + 110P^3 + 17P^4 + P^5)e^P E_1(P) \\
& + (-36 + 238P + 230P^2 + 95P^3 + 16P^4 + P^5),
\end{aligned} \tag{69}$$

$$\begin{aligned}
d_4(P) = & (48 + 288P + 552P^2 + 416P^3 + 138P^4 + 20P^5 + P^6)[e^P E_1(P)]^2 \\
& - 2(86 + 314P + 312P^2 + 120P^3 + 19P^4 + P^5)e^P E_1(P) \\
& + (150 + 224P + 103P^2 + 18P^3 + P^4),
\end{aligned} \tag{70}$$

and

$$\begin{aligned}
e_4(P) = & 4P^{3/2} \left[e^P E_1(P)(2 + 4P + P^2) - (3 + P) \right] \\
& \left[e^P E_1(P)(6 + 18P + 9P^2 + P^3) - (11 + 8P + P^2) \right].
\end{aligned} \tag{71}$$

6 Shapes in Cylindrical Coordinates

To facilitate comparison with experiment, we express our dendrite shapes for $n = 2, 3$, and 4 in cylindrical coordinates as $z = g(r, \phi) = P/2 - r^2/(2P) + \epsilon g^{(1)}(r, \phi) + \epsilon^2 g^{(2)}(r, \phi)/2 + O(\epsilon^3)$. In the previous section these shapes are given in parabolic coordinates by equations of the

form $\xi = f(\eta, \phi) = \xi_0 + \epsilon f^{(1)}(\eta, \phi) + \epsilon^2 f^{(2)}(\eta, \phi)/2 + O(\epsilon^3)$. For all n , $f^{(1)}$ is given by Eq. (38), whereas $f^{(2)}$ is given by Eqs. (27), (56), and (68) for $n = 2, 3$, and 4 , respectively. To convert these expressions to cylindrical coordinates we use Eqs. (5)–(7) to relate the coordinates η and ϕ on the dendrite surface $\xi = f(\eta, \phi)$ to the coordinates r and ϕ on the same surface expressed in the form $z = g(r, \phi)$, and expand the relations term by term in ϵ through second order.

For the Horvay-Cahn solution with $n = 2$ this gives the shape

$$\frac{z}{P} = \frac{1}{2} - \frac{1}{2} \left(\frac{r}{P}\right)^2 - \frac{\epsilon}{2} \cos 2\phi \left(\frac{r}{P}\right)^2 - \frac{\epsilon^2}{2} \left(\frac{r}{P}\right)^2 + O(\epsilon^3). \quad (72)$$

For $n = 3$ the corresponding shape is given by

$$\frac{z}{P} = \frac{1}{2} - \frac{1}{2} \left(\frac{r}{P}\right)^2 - \frac{\epsilon}{2} \cos 3\phi \left(\frac{r}{P}\right)^3 - \frac{\epsilon^2}{2} \left[P^{1/2} c_3 \left(\frac{r}{P}\right)^4 \right] + O(\epsilon^3). \quad (73)$$

The results for $n = 4$ are

$$\frac{z}{P} = \frac{1}{2} - \frac{1}{2} \left(\frac{r}{P}\right)^2 - \frac{\epsilon}{2} \cos 4\phi \left(\frac{r}{P}\right)^4 + \frac{\epsilon^2}{2} \left[\frac{P^{1/2} c_4}{e_4} \left(\frac{r}{P}\right)^4 - \frac{P^{3/2} d_4}{e_4} \left(\frac{r}{P}\right)^6 \right] + O(\epsilon^3), \quad (74)$$

The latter expression is equivalent to that given in Eq. (3) with the definitions $\alpha = P^{1/2} c_4/e_4$ and $\beta = -P^{3/2} d_4/e_4$.

We note that the Horvay-Cahn shape for $n = 2$ represents a relative correction that grows no faster than the unperturbed shape ($\epsilon = 0$) as $r \rightarrow \infty$. The shapes for $n = 3$ and $n = 4$ have corrections that grow faster than the unperturbed shape, and must be interpreted as providing a local solution near the tip that should be “matched” to another solution that is valid in the far field in order to obtain a uniformly valid solution (see, e.g., Ref. [12]). We also note that there are no $O(\epsilon^2)$ non-axisymmetric corrections to the shape in cylindrical coordinates, in contrast to the corrections found using parabolic coordinates; cf. Eqs. (27), (56), and (68).

Solvability theory [12] assumes a three-dimensional dendrite tip which can be expressed in the form

$$\frac{z}{\rho} = \frac{1}{2} - \frac{1}{2} \left(\frac{r}{\rho}\right)^2 + \sum_{n \geq 1} A_{4n} \left(\frac{r}{\rho}\right)^{4n} \cos 4n\phi. \quad (75)$$

for growth of cubic materials about a four-fold axis. Solvability results based on this expres-

sion provide estimates of the magnitude of the four-fold shape perturbation for SCN that are too high by a factor of three [12–14]. Since the isothermal expansion results that we have obtained include additional axisymmetric contributions that are not included in the shape that is assumed in the solvability theory, it would be interesting to consider the effects of basing the solvability analysis on our second-order isothermal solution with four-fold symmetry.

7 Comparison with Shape Measurements

Glicksman et al. [3] have measured the function $Q(\phi)$ that appears in Eq. (2) for a supercooling of 0.46 K, which corresponds to $P \approx 0.004$. Their measurements (see Figure 10 of [3]) lead to the approximate result

$$Q(\phi) \approx -0.004 \cos 4\phi, \quad (76)$$

in terms of the main harmonic; the data suggest that higher harmonics are likely to be significant as well. Here, the orientation $\phi = 0$ corresponds to the [100] direction. Comparison with Eq. (3) to order ϵ results in $\epsilon \approx -0.008$. For $P = 0.004$, the expression (65) for $S^{(2)}$ gives $S^{(2)} = 56.6$ so that the correction $\epsilon^2 S^{(2)}/2 = 1.8 \times 10^{-3}$ in Eq. (4) is actually about 9 % of the unperturbed value of $S^{(0)} = 0.02$. This result is in good accord with the measured deviations from the Ivantsov result shown in Fig. 6 of Ref. [2].

We now use the values $P = 0.004$ and $\epsilon = -0.008$ to explore the shape predicted by Eq. (3), which in dimensional variables becomes

$$\frac{z}{\rho} = \frac{1}{2} - \frac{1}{2} \left(\frac{r}{\rho}\right)^2 + 0.004 \cos 4\phi \left(\frac{r}{\rho}\right)^4 - 0.0004 \left(\frac{r}{\rho}\right)^4 - 0.00003 \left(\frac{r}{\rho}\right)^6, \quad (77)$$

Given that the $(r/\rho)^6$ terms make this shape more complicated than that used by Glicksman et al. to fit their data, and also given the fact that higher harmonics [viz. $\cos 8\phi$] are apparent in their data, it is not possible to make a more quantitative comparison at this stage. Note that for $r/\rho \sim 4$, which is typical of the range of their measurements, the axially-symmetric sixth order and fourth order terms are comparable in magnitude.

In Fig. 6 we show a three-dimensional view of the dendrite shape obtained by using the representation in parabolic coordinates as given by Eqs. (38) and (68) with $P = 0.004$ and

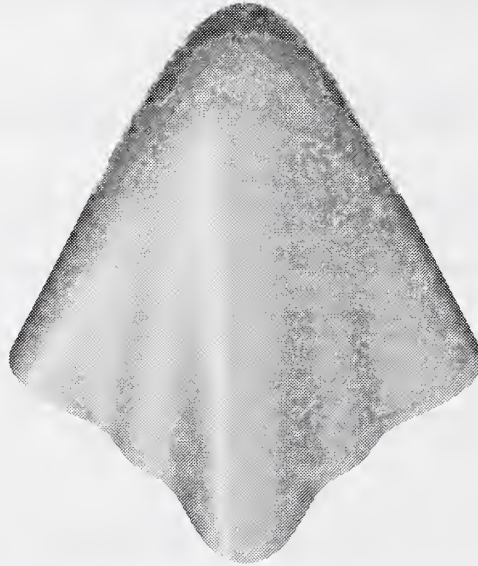


Figure 6: A three-dimensional view of the non-axisymmetric isothermal dendrite.

$\epsilon = -0.008$. To emphasize the deviations from the axisymmetric shape with $\epsilon = 0$ due to the higher order contributions, we have plotted the shape out to a value $z/\rho = 25$, which is well beyond the formal range of validity of the expansion. (Far from the tip, the corrections become large in magnitude, and the form of the corrections in parabolic and cylindrical coordinates are not equivalent.)

8 Discussion

We have obtained approximate solutions for dendrite shapes having three and four fold sinusoidal axial anisotropies of amplitude of order ϵ . These shapes lead to corrections of order ϵ^2 to the Ivantsov relationship between the Peclet number P and the Stefan number

S . To second order in ϵ , these solutions satisfy the flux condition at the surface of an assumed isothermal dendrite. Insofar as the relationship between P and S is concerned, the assumption of isothermality should be valid at low supercoolings where the tip radius ρ of the dendrite is relatively large. From Ref. [3], the measured tip radius for the supercooling of 0.46 K that we have studied here is $\rho = 25\mu\text{m}$, which leads to a capillary correction of $2T_M\gamma/(L_V\rho) = 5\text{ mK}$, where we have used a value $T_M\gamma/L_V = 6.19 \times 10^{-6}\text{ K cm}$ [24].

The matter of the selection of ρ itself is critically dependent on capillarity as expressed through the Gibbs-Thomson equation. For that matter, the value of ϵ is also dependent on capillarity, and is subject to a selection criterion as discussed by Brener et al. [12–14] who obtain a prediction for ϵ that is a factor of three larger than the measured value for SCN. From Fig. 5 we note that the correction factor $S^{(2)}/S^{(0)}$ decreases as P increases. The dependence of ϵ on Peclet number has not been studied extensively. Preliminary measurements by LaCombe over a small range of supercoolings suggest that there is not a strong dependence of ϵ on Peclet number [16]. Shape measurements on ammonium bromide dendrites have been made by Mauer et al. [22], who find that $|\epsilon| \approx 0.05$ for a range of conditions leading to dendrites with tip radii in the range of 1 to 4 μm . Bisang and Bilgram [5] have studied the shape of the four-fold protruding fins in the [001] directions for xenon dendrites, finding that a power law fit is superior to a polynomial fit over a large range of distances from the tip. Karma and Rappel [23] compute shape corrections based on three-dimensional numerical simulations of dendritic growth using a phase-field model. They consider growth at a supercooling of $S = 0.45$, and compute the variation of the Peclet number and ϵ with the degree of surface tension anisotropy in the model. The Peclet number varies from 0.43 to 0.09 and ϵ varies from 0.02 to 0.06 as the magnitude of the anisotropy is increased. Whereas, for $S = 0.45$, the value of the Peclet number is $P = 0.47$, based on the Ivantsov solution ($\epsilon = 0$). Our results based on an isothermal dendrite predict a much smaller correction at these supercoolings (see Fig. 5), suggesting that the isothermal approximation is not valid for these large supercoolings.

The solutions that we have obtained might provide a better basis than the Ivantsov solution for considerations of a selection criteria for ρ , V , and the amplitudes of the non-axisymmetric components of the shape. The procedure that we have used can also be extended to obtain solutions for shapes having six-fold or eight-fold axial symmetry, either as independent solutions in their own right or as harmonic corrections to our three-fold and four-fold solutions.

9 Acknowledgments

We thank M. E. Glicksman, M. B. Koss, and J. C. LaCombe for helpful discussions. This work was conducted with the support of the Microgravity Research Division of NASA. RFS is grateful for support of the National Science Foundation, Grant DMR9634056.

References

- [1] M. E. Glicksman, S. P. Marsh, in Handbook of Crystal Growth 1 Fundamentals, Part B: Transport and Stability, ed. D. T. J. Hurle (North-Holland, Amsterdam, 1993) p. 1075.
- [2] M. E. Glicksman, M. B. Koss, L. T. Bushnell, Jeffrey C. LaCombe, E. A. Winsa, *ISIJ Int.* 35 (1995) 604.
- [3] J. C. LaCombe, M. B. Koss, V. E. Fradkov, M. E. Glicksman, *Phys. Rev. E.* 52 (1995) 2778.
- [4] M.B. Koss, L.T. Bushnell, J.C. LaCombe, M. E. Glicksman, *Chem. Eng. Comm.* 152-153 (1996) 351.
- [5] U. Bisang, J.H. Bilgram, *Phys. Rev. E* 54 (1996) 5309.
- [6] G. P. Ivantsov, *Dokl. Akad. Nauk SSSR* 58 (1947) 567.
- [7] J. S. Langer, *Rev. Mod. Phys.* 52 (1980) 1.
- [8] J. S. Langer, in *Le hasard et la matière/Chance and matter*, Les Houches, Session XLVI, Course 10, (North Holland, Amsterdam, 1987) pp. 629.
- [9] D.A. Kessler, H. Levine, *Phys. Rev. A* 36 (1987) 4123.
- [10] David A. Kessler, Joel Koplik and Herbert Levine, *Advances in Physics* 37, 255 (1988).
- [11] E. A. Brener, V.I. Mel'nikov, *Advances in Physics* 40, 53 (1991).
- [12] M. Ben Amar, E. Brener, *Phys. Rev. Lett.* 71 (1993) 589.
- [13] E. Brener, *Phys. Rev. Lett.* 71 (1993) 3653.
- [14] E. Brener, V.I. Mel'nikov, *JETP* 80 (1995) 341.
- [15] R.J. Schaefer, *J. Crystal Growth* 43 (1978) 17.
- [16] J.C. LaCombe, Ph. D. Thesis, Department of Materials Science and Engineering, Rensselaer Polytechnic Institute, Troy, NY, December, 1998.
- [17] G. Horvay, J. W. Cahn, *Acta Met.* 9 (1961) 695.

- [18] S.-K. Chan, H.-H. Reimer, and M. Kahlweit, *J Crystal Growth* **32**, 303 (1976).
- [19] M.F. Henry, Y.S. Yoo, D.Y. Yoon, and J. Choi, *Metall. Trans.* **24A**, 1733 (1993).
- [20] W. Magnus, F. Oberhettinger, *Formulas and Theorems for the Functions of Mathematical Physics*, (Chelsea Publishing Co., New York, 1949).
- [21] M. Abramowitz, I. A. Stegun, *Handbook of Mathematical Functions*, Applied Mathematics Series 55, National Bureau of Standards, Washington, 1964.
- [22] J. Mauer, B. Perrin, P. Tabeling, *Europhys. Lett.* **14** (1991) 575.
- [23] A. Karma, W.-J. Rappel, *Phys. Rev. E* **57** (1998) 4342.
- [24] R.J. Schaefer, M.E. Glicksman, J.D. Ayers, *Phil. Mag.* **32** (1975) 725.

Appendix: Exact Solutions with n-Fold Symmetry

If we look for a solution of the form

$$T(\xi, \eta, \phi) = \frac{e^{-\xi^2}}{\xi^2 + \eta^2} g(\eta/\xi) \cos n\phi, \quad (78)$$

and set $\zeta = \eta/\xi$, then $g(\zeta)$ is found to satisfy

$$\zeta^2 g_{\zeta\zeta} + \zeta g_{\zeta} - n^2 g = 0. \quad (79)$$

This equation is homogeneous in ζ with solutions $g(\zeta) = \zeta^\alpha$, where we find two solutions $\alpha = \pm n$ for nonzero n . For $n = 0$, the solution has the form

$$g(\zeta) = A + B \log \zeta. \quad (80)$$

For $n = 4$, there are solutions of the form

$$T(\xi, \eta, \phi) = \frac{e^{-\xi^2}}{\xi^2 + \eta^2} \left\{ A \left(\frac{\xi}{\eta} \right)^4 + B \left(\frac{\eta}{\xi} \right)^4 \right\} \cos 4\phi. \quad (81)$$

In the original Cartesian coordinate system, it is clear that a z -derivative of a solution to the partial differential equation is also a solution. By using the relations

$$\xi_z = \frac{\xi}{(\xi^2 + \eta^2)}, \quad \eta_z = \frac{-\eta}{(\xi^2 + \eta^2)}, \quad (82)$$

the z -derivative of the n -fold solution,

$$T(\xi, \eta, \phi) = \frac{e^{-\xi^2} \cos n\phi}{(\xi^2 + \eta^2)} \left(\frac{\eta}{\xi} \right)^n, \quad (83)$$

is given by

$$\frac{\partial T}{\partial z}(\xi, \eta, \phi) = \frac{-2e^{-\xi^2} \cos n\phi}{(\xi^2 + \eta^2)^3} \left(\frac{\eta}{\xi} \right)^n [\xi^4 + \xi^2\eta^2 + (n+1)\xi^2 + (n-1)\eta^2]. \quad (84)$$

This solution, taken with $2n$ -fold symmetry, is used to provide the non-axisymmetric second order correction in the perturbation expansion of the n -fold solution; see, e.g. Eq. (41).

We note that $E_1(\xi^2)$ is a solution,

$$\frac{\partial}{\partial z} E_1(\xi^2) = -2 \frac{e^{-\xi^2}}{(\xi^2 + \eta^2)} \quad (85)$$

is also a solution, and

$$\frac{\partial^2}{\partial z^2} E_1(\xi^2) = 4 \frac{e^{-\xi^2}}{(\xi^2 + \eta^2)^3} [\xi^2(\xi^2 + \eta^2) + \xi^2 - \eta^2] \quad (86)$$

is also a solution.

To solve the n -fold problem with $n > 2$ we need additional axisymmetric solutions that have more rapid growth in η as $\eta \rightarrow \infty$. These solutions are obtained by integration of $E_1(\xi^2)$, rather than by differentiation. The equation

$$\frac{\partial}{\partial z} w(\xi, \eta) = \xi_z w_\xi + \eta_z w_\eta = F(\xi, \eta) \quad (87)$$

takes the form of a first order partial differential equation,

$$\xi w_\xi - \eta w_\eta = (\xi^2 + \eta^2) F(\xi, \eta) \quad (88)$$

which can be solved using the method of characteristics. The solution satisfies an ordinary differential equation along the characteristic curve $\xi\eta = \xi_0\eta_0$ that issues from the point (ξ_0, η_0) along the initial surface $\xi = \xi_0 = P^{1/2}$. The solution that decays as $\xi \rightarrow \infty$ can be

given in terms of the function

$$w_0(\xi, \eta_0) = - \int_{\xi}^{\infty} \left[\lambda + \frac{\eta_0^2 \xi^2}{\lambda^3} \right] F(\lambda, \eta_0 \xi_0 / \lambda) d\lambda, \quad (89)$$

by substituting $\eta_0 = \eta \xi / \xi_0$ to give $w(\xi, \eta) = w_0(\xi, \eta \xi / \xi_0)$. For $F(\xi, \eta) = E_1(\xi^2)$, this gives a solution

$$u(\xi, \eta) = \frac{1}{2}(\eta^2 - 1)e^{-\xi^2} + \frac{1}{2}(\xi^2 - \xi^2 \eta^2 - \eta^2)E_1(\xi^2), \quad (90)$$

which can be seen to satisfy $u_z = E_1(\xi^2)$. The function u grows quadratically in η for fixed ξ .

We also compute a solution $v(\xi, \eta)$ to the problem $v_z = u$. This solution takes the form

$$\begin{aligned} v(\xi, \eta) &= \frac{1}{16}[2 + 4\xi^2 \eta^2 - 2\xi^2 + 4\eta^2 - \xi^2 \eta^4 - 3\eta^4]e^{-\xi^2} \\ &+ \frac{1}{16}[2\xi^4 + 2\eta^4 - 8\xi^2 \eta^2 - 4\xi^4 \eta^2 + 4\xi^2 \eta^4 + \xi^4 \eta^4]E_1(\xi^2). \end{aligned} \quad (91)$$

Both $u(\xi, \eta)$ and $v(\xi, \eta)$ are solutions of the partial differential equation (11).

